JMEPEG (2008) 17:708–713
DOI: 10.1007/s11665-008-9222-8

1059-9495/$19.00

Effect of Micro Arc Oxidation Coatings on Corrosion Resistance of 6061-Al Alloy

Nitin P. Wasekar, A. Jyothirmayi, L. Rama Krishna, and G. Sundararajan

(Submitted June 14, 2007; in revised form January 8, 2008)

In the present study, the corrosion behavior of micro arc oxidation (MAO) coatings deposited at two current densities on 6061-Al alloy has been investigated. Corrosion in particular, simple immersion, and potentiodynamic polarization tests have been carried out in 3.5% NaCl in order to evaluate the corrosion resistance of MAO coatings. The long duration (up to 600 h) immersion tests of coated samples illustrated negligible change in weight as compared to uncoated alloy. The anodic polarization curves were found to exhibit substantially lower corrosion current and more positive corrosion potential for MAO-coated specimens as compared to the uncoated alloy. The electrochemical response was also compared with SS-316 and the hard anodized coatings. The results indicate that the overall corrosion resistance of the MAO coatings is significantly superior as compared to SS316 and comparable to hard anodized coating deposited on 6061 Al alloy.

Keywords Al_2O_3 coating, corrosion, hard anodizing, micro arc oxidation, potentiodynamic polarization

1. Introduction

Micro arc oxidation (MAO) is an emerging ecofriendly coating technique capable of forming ceramic coatings on metals such as Al, Mg, Ti, and their alloys (Ref 1-5). The ceramic coatings deposited using MAO technique exhibit superior tribological properties (Ref 6-9). Previous studies on MAO coatings have been mostly devoted to the synthesis, analysis, and tribological behavior of these coatings (Ref 7-11). Much of the corrosion-related studies have been confined to MAO coatings formed on Mg and Ti alloys substrate (Ref 12-15). However, there exist a few studies investigating the corrosion behavior of MAO coatings, formed on Al alloys (Ref 16-18). Kuhn (Ref 16) demonstrated the improved corrosion resistance of MAO coatings compared to hard anodized coatings under salt spray test conditions. Nie et al. (Ref 17) studied the corrosion properties of 250-μm-thick MAO coating deposited at 0.1 A/cm^2 on BS 6082 Al alloy for different immersion periods in 0.5 M NaCl solution up to 48 h. Though the presence of occluded porosity in the MAO coating was confirmed by TEM, it did not affect the corrosion resistance. Recent study by Barik et al. (Ref 18) illustrates the importance of sealing the pores in MAO coatings by sol–gel technique in enhancing the short-term corrosion resistance in 0.6 M NaCl solution. The above investigation also revealed that the MAO coatings (unsealed) did not improve the corrosion resistance of Al alloy because of the presence of through thickness coating defects. Thus, there exist conflicting data on the effectiveness of MAO coatings formed on Al alloys against the aqueous corrosion.

It has already been demonstrated that the current density plays a significant role on the MAO coating deposition kinetics and development (Ref 7, 10). It has been found that α-alumina content increases with an increase in current density in MAO coatings (Ref 19). So far the effect of current density on long-term corrosion behavior of MAO coatings deposited on Al alloys has not been studied. Moreover, a recent study by Curran et al. (Ref 20) found that the MAO coatings characterized by up to 20% of surface connected porosity which is expected to substantially influence the corrosion properties of the coatings. The MAO coatings deposited at the author's laboratory were found to be dense and have exhibited excellent tribological properties (Ref 7, 21). However, the corrosion properties of these coatings need to be studied in order to establish the suitability of these coatings for applications requiring corrosion resistance in addition to wear resistance.

In the view of above, the major objective of the present study is to evaluate the overall effectiveness of MAO coatings in terms of resistance to aqueous corrosion. Toward the above objective, MAO coatings have been deposited on a 6061 Al alloy at current densities of 0.1 and 0.3 A/cm^2 and their corrosion behavior evaluated in 3.5% NaCl solution. The corrosion resistance has been evaluated using weight loss (immersion) and the potentiodynamic polarization technique. In addition, the corrosion performance of MAO coatings has been compared with hard anodized coatings deposited on 6061 Al alloy as well as SS316L.

2. Experimental Details

2.1 MAO Coating Procedure

A 6061-T6 Al alloy having the nominal composition 1.1% Mg, 0.7% Si, 0.1% Cu, 0.6% Fe, 0.15% Mn, 0.2% Zn, 0.016% Ti,

Nitin P. Wasekar, A. Jyothirmayi, L. Rama Krishna, and **G. Sundararajan**, International Advanced Research Centre for Powder Metallurgy and New Materials (ARCI), Balapur (P.O.), Hyderabad 500005, India. Contact e-mail: nitin.arci@gmail.com.

and balance Al was used as the substrate material for MAO coating deposition in the present study.

MAO coatings were deposited in an alkaline electrolytic bath containing potassium hydroxide and sodium silicate. A 70 kVA MAO coating deposition unit designed and built in the authors' laboratory was used for the coating deposition. The electrolyte was continuously circulated in the reaction chamber made of non-conductive material. The bath temperature was maintained at 16-18 °C with the help of an external heat exchanger. The samples to be coated were immersed in the electrolyte and the specially regulated power was supplied to achieve the coating deposition. The detailed description of the equipment and the electrical waveforms employed are given in Ref 22. The coating deposition was carried out at two different current densities (0.1 and 0.3 A/cm^2) on 25-mm diameter and 5-mm-thick 6061 Al alloy coupons. Prior to coating deposition, the coupons were ultrasonically cleaned in acetone. The coating deposition time was adjusted in such a way that the final coating thickness was in the range of 50 ± 5 μm. After coating deposition the samples were taken out of bath and rinsed in running water, and then dried in hot air. In addition to comparative evaluation of corrosion resistance, SS-316L and hard anodized coatings (thickness 50 ± 5 μm) deposited on 6061 Al alloy samples were employed.

2.2 MAO Coating Characterization

The coatings were subjected to X-ray diffractometry (D8-Advance, Brooker, Germany, CuKα radiation, Bragg-Brenton geometry, 40 kV, 40 mA, 0.02°/s scan rate) to identify different phases present. The coating morphology of samples was studied using scanning electron microscopy (Hitachi Model S-4300SE/N, Japan). Energy dispersion spectroscopy (EDS) was carried out to perform spectral analysis using the Genesis Software of EDAX.

2.3 Evaluation of Corrosion Resistance

Immersion tests were carried out in 3.5% NaCl solution for 1, 24, 48, 168, and 600 h and weight change was measured for both uncoated and MAO-coated coupons. In addition, for a detailed study of the nature of corrosion as a function of immersion period, the electrochemical response was evaluated on samples exposed to different periods up to 600 h. For such an electrochemical testing, a Solartron 1260 Impedance/Gain Phase analyzer with a Solartron 1287 Electrochemical Interface was used to generate the E vs. log(i) plots. The MAO-coated and bare Al alloy coupons were exposed to 3.5% NaCl solution for different exposure periods (1-600 h). A 3-electrode potentiostatic mode was applied with a saturated calomel reference electrode (SCE). Platinum electrode was used as a counter electrode. Polarization tests were carried out using Corrware and Corrview software at a scan rate of 1 mV/s. The polarization resistance values were calculated using Stern-Geary equation (Ref 23) using Eq. 1.

$$R_p = \left\{ \frac{(\beta_{anodic})(\beta_{cathodic})}{2.303(\beta_{anodic} + \beta_{cathodic})} \right\} (1/I_{corr}) \quad \text{(Eq 1)}$$

where I_{corr} is the corrosion current density (A/cm^2), β_{anodic} is the anodic Tafel slope (mV/decade), and $\beta_{cathodic}$ is the cathodic Tafel slope (mV/decade).

3. Results and Discussion

3.1 Coating Morphology and Phase Composition

The SEM micrographs of the MAO coating surface are shown in Fig. 1(a)-(c). The coating surface is composed of discharge channels which are seen at higher magnification as a pancake structure (Fig. 1b) with the indication of material flow

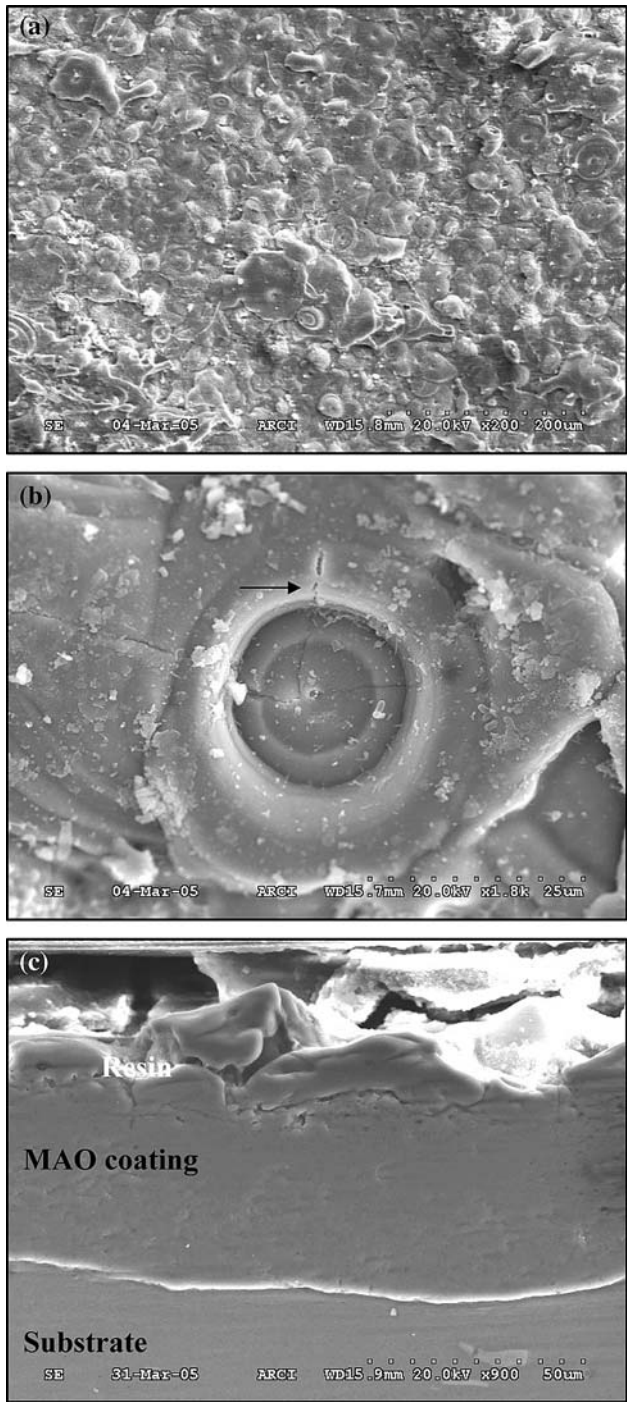

Fig. 1 SEM surface morphology of (a) typical MAO coating, (b) discharge channel with cracks due to thermal stresses, and (c) cross section of MAO coating

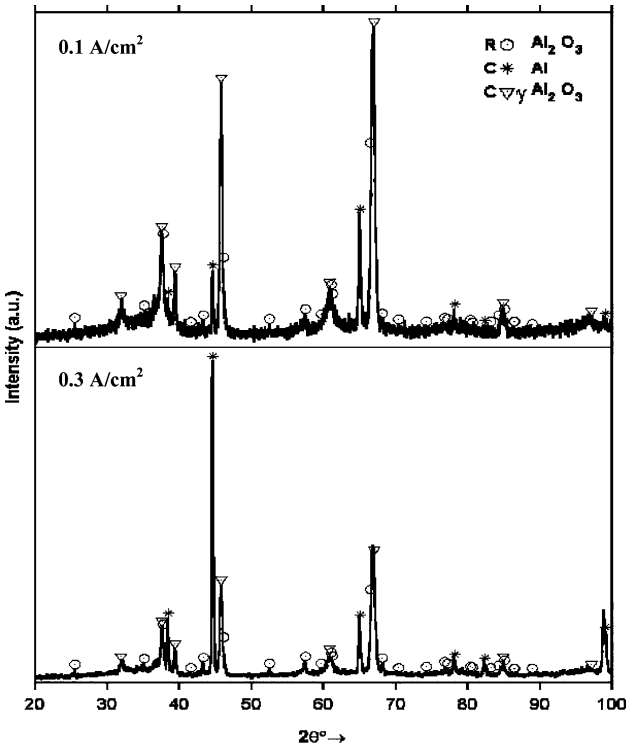

Fig. 2 XRD patterns of MAO coatings deposited at 0.1 and 0.3 A/cm^2 illustrating crystalline α-Al_2O_3 (○) and γ-Al_2O_3 (inverted Δ) as major phases

out of these circular channels on to the coating surface all along the periphery. The cross-sectional view of the MAO coatings formed on the 6061 Al alloy is shown in Fig. 1(c). A clear interface without cracks can be observed between the coating and the substrate.

The X-ray diffraction spectrum obtained on the MAO coatings deposited at a current density of 0.1 and 0.3 A/cm^2 is shown in Fig. 2. It is clear that both α-Al_2O_3 and γ-Al_2O_3 are present as major phases in the MAO coatings formed at both current densities. This result is consistent with the results obtained in earlier studies (Ref 2, 10, 11).

3.2 Corrosion Behavior

3.2.1 Immersion Tests. The results from the immersion tests in 3.5% NaCl solution carried out for different periods up to 600 h (25 days) are shown in Fig. 3 for MAO-coated and bare 6061 Al alloy. The bare alloy experienced a substantial weight loss immediately upon immersion fallowed by a slower weight loss increasing linearly with the immersion period. In contrast, the MAO-coated 6061 alloy (at both 0.1 and 0.3 A/cm^2) did not exhibit measurable weight loss (or gain) up to a period of 48 h. Even beyond this period, the weight loss suffered by the MAO-coated Al alloy is substantially lower than the bare alloy. However, among the MAO-coated samples, the one coated at the current density 0.1 A/cm^2 exhibits a marginally lower weight loss as compared to the samples coated at 0.3 A/cm^2. If the slope of linear part of the weight loss–immersion period curves are considered as a reflection of the corrosion rate during immersion in 3.5% NaCl, the bare alloy exhibits a corrosion rate 1.36 μg/cm^2 h while the MAO-coated Al alloy samples exhibit corrosion rate of 0.19 μg/cm^2 h

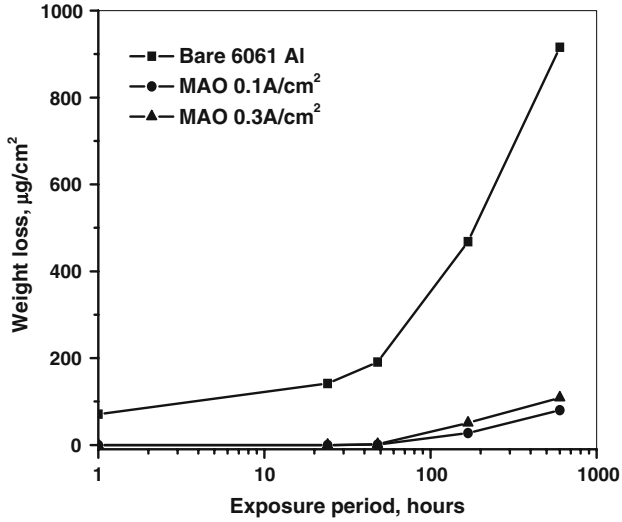

Fig. 3 Immersion test results illustrating the weight loss as a function of immersion period for MAO coatings and bare alloy in 3.5% NaCl solution

and 0.14 μg/cm^2 h for the coatings deposited at a current density of 0.3 and 0.1 A/cm^2, respectively. The macroscopic examination of the MAO-coated Al alloy after immersion in 0.5 M NaCl for 600 h did not reveal any obvious corrosion damage.

However, the examination of the MAO-coated samples after 600 h of immersion at a higher magnification using SEM did reveal the presence of discrete, microscopic spots where corrosion had initiated. Figure 4 illustrates the SEM micrograph of these corrosion spots in MAO coating immersed for a period of 600 h in 3.5% NaCl solution. A closer examination of the corrosion spot reveals a granular deposit. An analysis of these corrosion products by EDS reveals that it is composed of elements Al, O, Cl, and Na (Fig. 4b). On the basis of the above data in conjunction with the earlier work (Ref 24, 25); it is likely that the corrosion product is essentially boehmite (i.e., $Al_2O_3.3H_2O$). Thus, it can be concluded that MAO coatings do undergo microscopic corrosion damage at longer immersion periods.

3.2.2 Polarization Tests. The polarization curves pertaining to bare and MAO-coated 6061 alloy as a function of immersion period in NaCl solution are illustrated in Fig. 5(a)-(d). The variation of corrosion potential (E_{corr}) and corrosion current (I_{corr}) as a function of immersion period for bare and MAO-coated 6061 alloy, as evaluated from Fig. 5, are presented in Fig. 6(a) and (b), respectively. A perusal of Fig. 5 and 6 indicates the following:

1. The corrosion potential is more noble for MAO-coated 6061 alloy as compared to bare 6061 alloy up to an immersion period of 168 h. However, after 600 h of immersion, the corrosion potential of MAO coatings is less noble than that of bare 6061 alloy. This is most probably due to the fact that at discrete locations wherein the electrolyte has penetrated the MAO coating after long immersion duration to cause corrosion of Al alloy substrate, the resulting corrosion product (i.e., $Al(OH)_{3-x}Cl_x$) in chloride containing electrolyte causes liberation of hydroxyl ions, thereby increasing the electrolyte pH in

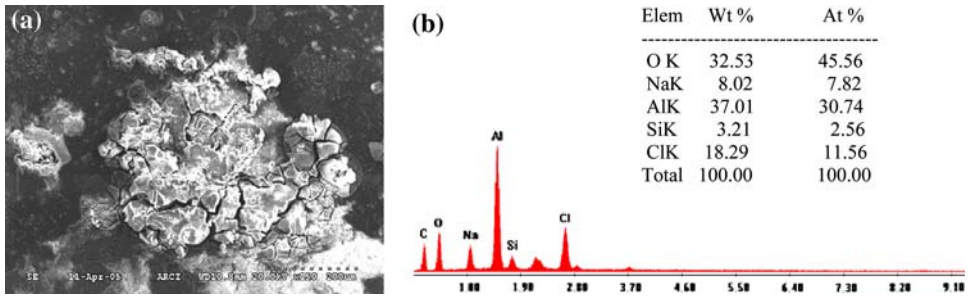

Fig. 4 SEM micrographs (a) and EDS spectra (b) of MAO coating deposited at 0.1 A/cm^2 after 25 days of exposure of 3.5% NaCl solution showing corrosion product formation and presence of various elements in the corrosion product

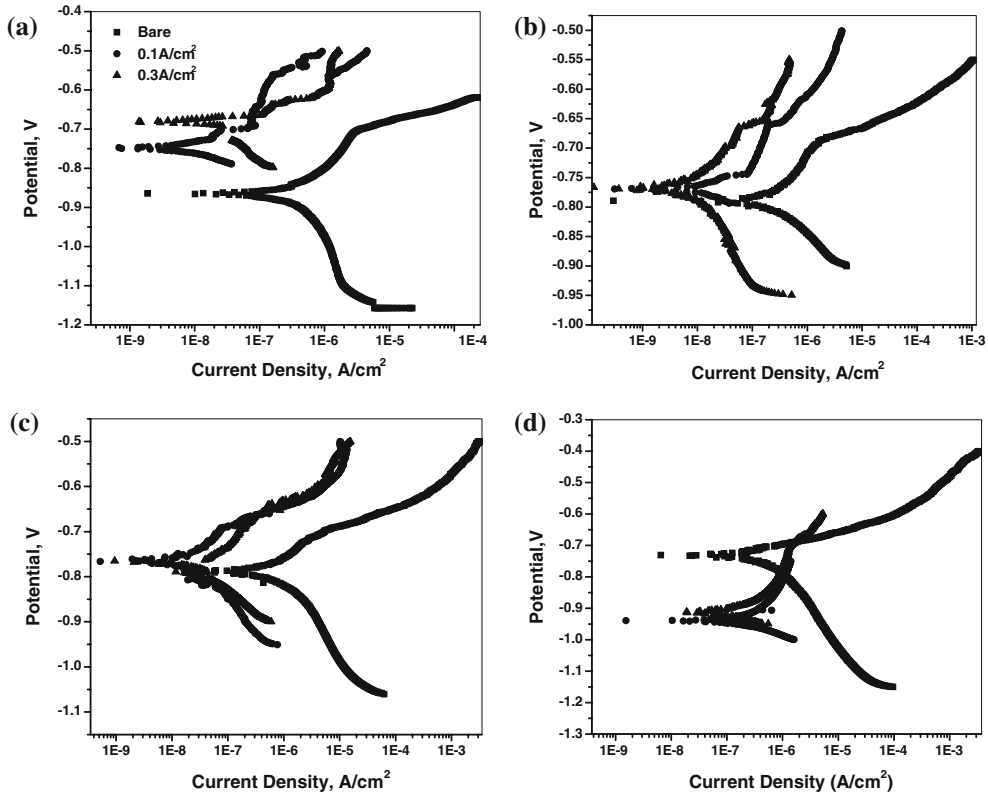

Fig. 5 Polarization curves for bare substrate, MAO-coated 6061 Al alloy after immersion in 3.5% NaCl solution for different periods: (a) 1 h, (b) 48 h, (c) 168 h, and (d) 600 h

the local region (Ref 26). Such an increase in alkanity, as is well known (Ref 27, 28), increases the corrosion potential toward more active values as observed experimentally.

2. The corrosion current values of MAO-coated 6061 alloy are considerably lower than that of the bare alloy at all immersion periods up to 600 h.
3. MAO coatings formed at current densities of 0.1 and 0.3 A/cm^2 exhibit nearly identical behavior with respect to variation of corrosion potential and current with immersion period.

On the basis of the above observations, it can be concluded that MAO coatings do confer substantial protection to 6061 Al alloy with regard to corrosion in 3.5% NaCl solution, at least up to an immersion period of 600 h.

3.2.3 Comparative Corrosion Studies. Figure 7 illustrates the polarization tests results for MAO-coated 6061 Al, 6061 Al substrate; Hard anodized 6061 Al and Stainless Steel-316 L after 1-h exposure to 3.5% NaCl solution. MAO coating exhibited corrosion potential more noble than bare Al alloy and also hard anodized alloy. Due to the intrinsic property of SS 316 alloy in particular, the formation of Cr_2O_3 passive layer, the corrosion potential (Ref 29) was more noble than the Al alloy substrate as well as MAO and hard anodized coatings. The corrosion rate is normally indicated in terms of the corrosion current calculated as per Eq. 1 using Tafel slopes from Fig. 7 and are compared in Table 1. It is clear from Table 1 that MAO coating exhibits the lowest corrosion current values as compared to substrate, hard anodized coating and even SS 316 alloy probably as a result of the dense Al_2O_3 coatings formed on Al alloy substrate through MAO technique. In contrast, hard

anodized coatings are known to exhibit through-thickness pores with a relatively thin barrier layer at the pore base (Ref 30, 31) and thus these coatings allow the interaction of the corrosion media with the substrate at relatively shorter immersion periods. On the other hand, the stainless steel is well known to be a noble material due to its passivation and thus exhibits a more positive corrosion potential as compared to the coatings and the bare substrate (Fig. 7). However, in the presence of Cl^- ions the passive layer formed on stainless steel is readily destroyed, leading to very high corrosion rates.

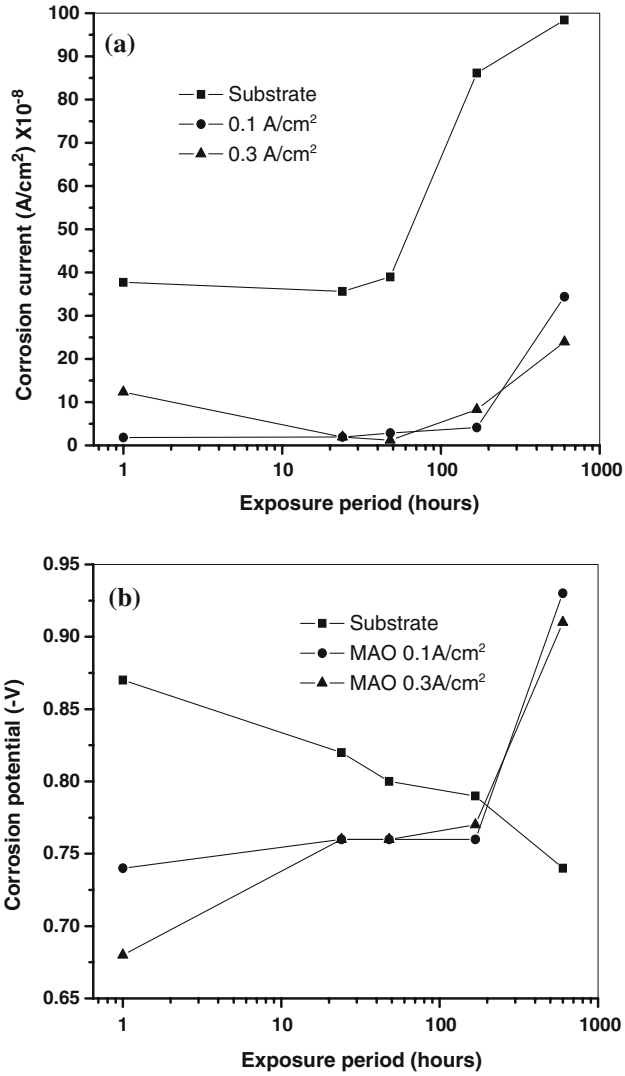

Fig. 6 (a) Corrosion current (I_{corr}) and (b) corrosion potential (E_{corr}) as a function of exposure period in 3.5% NaCl solution

4. Conclusions

The main conclusions of the present study are:

1. The weight loss encountered by MAO coatings and bare substrate during the immersion tests in 3.5% NaCl solution increased with increase in immersion time. However, the weight loss suffered by the MAO coatings deposited at 0.1 A/cm^2 is 71 times lower than bare substrate after 1 h and 12 times lower than bare substrate after 600 h of immersion.
2. No visual evidence of pitting corrosion was found for the coatings deposited at both the current densities, 0.1 and 0.3 A/cm^2, even after 600 h exposure to 3.5% NaCl solution.
3. Polarization tests carried out up to 600 h of exposure to 3.5% NaCl solution demonstrated higher corrosion resistance of MAO coatings than bare Al alloy substrate. The corrosion rate was 4.5 times lower for MAO coatings after 1 h and 48 times lower after 600 h of exposure to salt solution than bare substrate.

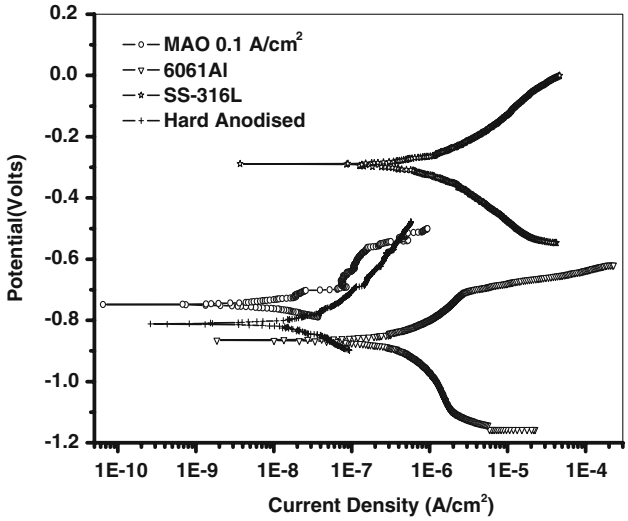

Fig. 7 Polarization curves for MAO-coated 6061 Al alloy, substrate, hard anodized 6061 Al alloy and SS-316L after 1 h exposure to 3.5% NaCl solution

Table 1 Potentiodynamic polarization test results after 1 h exposure to 3.5% NaCl solution

Sample	E_{corr} (mV)	I_{corr} (A/cm^2 × 10^{-8})	R_p^a (MΩ)	Corrosion rate (MPY)
6061 Al alloy substrate	–0.8664	37.74	0.07	0.162
MAO (0.1 A/cm^2)	–0.7476	1.79	1.46	0.007
MAO (0.3 A/cm^2)	–0.6811	12.31	0.21	0.054
SS-316	–0.291	81.5	0.032	0.334
Hard anodized 6061 Al	–0.811	2.89	0.902	0.012

[a]Polarization resistance

4. The results of polarization tests illustrated enhanced corrosion resistance of Al alloy substrate due to MAO coatings as compared to hard anodized coating as well as stainless steel 316 L substrate in 3.5% NaCl solution.

References

1. A.L. Yerokhin, A.A. Voevodin, V.V. Lyubimov, J. Zabinski, and M. Donley, Plasma Electrolytic Fabrication of Oxide Ceramic Surface Layers for Tribotechnical Purposes on Aluminium Alloys, *Surf. Coat. Technol.*, 1998, **110**(3), p 140–146
2. X. Nie, A. Leyland, H.W. Song, A.L. Yerokhin, S.J. Dowey, and A. Matthews, Thickness Effects on the Mechanical Properties of Micro-arc Discharge Oxide Coatings on Aluminium alloys, *Surf. Coat. Technol.*, 1999, **116–119**, p 1055–1060
3. S.V. Gnedenkov, O.A. Khrisanfova, A.G. Zavidnaya, S.L. Sinebrukhov, A.N. Kovryanov, T.M. Scorobogatova, and P.S. Gordienko, Production of Hard and Heat-Resistant Coatings on Aluminium Using a Plasma Micro-discharge, *Surf. Coat. Technol.*, 2000, **123**(1), p 24–28
4. Y.K. Wang, L. Sheng, R.Z. Xiong, and B.S. Li, Study of Ceramic Coatings Formed by Microarc Oxidation on Al Matrix Composite Surface, *Surf. Eng.*, 1999, **15**(2), p 112–114
5. P.I. Butyagin, Ye.V. Khokhryakov, and A.I. Mamaev, Microplasma Systems for Creating Coatings on Aluminium Alloys, *Mater. Lett.*, 2003, **57**(11), p 1748–1751
6. Y. Zhang, C. Yan, F. Wang, H. Lou, and C. Cao, Study on the Environmentally Friendly Anodizing of AZ91D Magnesium Alloy, *Surf. Coat. Technol.*, 2002, **161**(1), p 36–43
7. L. Rama Krishna, K.R.C. Somaraju, and G. Sundararajan, The Tribological Performance of Ultra-hard Ceramic Composite Coatings Obtained Through Microarc Oxidation, *Surf. Coat. Technol.*, 2003, **163–164**, p 484–490
8. A.A. Voevodin, A.L. Yerokhin, V.V. Lyubimov, M.S. Donley, and J.S. Zabinski, Characterization of Wear Protective Al-Si-O Coatings Formed on Al-based Alloys by Micro-arc Discharge Treatment, *Surf. Coat. Technol.*, 1996, **86–87**(2), p 516–521
9. J. Tian, Z. Luo, S. Qi, and X. Sun, Structure and Antiwear Behavior of Micro-arc Oxidized Coatings on Aluminum Alloy, *Surf. Coat. Technol.*, 2002, **154**(1), p 1–7
10. G. Sundararajan and L. Rama Krishna, Mechanisms Underlying the Formation of Thick Alumina Coatings Through the MAO Coating Technology, *Surf. Coat. Technol.*, 2003, **167**(2–3), p 269–277
11. A.L. Yerokhin, L.O. Snizhko, N.L. Gurevina, A. Leyland, A. Pilkington, and A. Matthews, Discharge Characterization in Plasma Electrolytic Oxidation of Aluminium, *J. Phys. D: Appl. Phys.*, 2003, **36**, p 2110–2120
12. L.O. Snizhko, A.L. Yerokhin, A. Pilkington, N.L. Gurevina, D.O. Misnyankin, A. Leyland, and A. Matthews, Anodic Processes in Plasma Electrolytic Oxidation of Aluminium in Alkaline Solutions, *Electrochim. Acta*, 2004, **49**(13), p 2085–2095
13. A.L. Yerokhin, X. Nie, A. Leyland, and A. Matthews, Characterisation of Oxide Films Produced by Plasma Electrolytic Oxidation of a Ti–6Al–4V Alloy, *Surf. Coat. Technol.*, 2000, **130**(2–3), p 195–206
14. Z. Yao, Z. Jiang, S. Xin, X. Sun, and X. Wu, Electrochemical Impedance Spectroscopy of Ceramic Coatings on Ti–6Al–4V by Micro-plasma Oxidation, *Electrochim. Acta*, 2005, **50**(16–17), p 3273–3279
15. H. Duan, K. Du, C. Yan, and F. Wang, Electrochemical Corrosion Behavior of Composite Coatings of Sealed MAO Film on Magnesium Alloy AZ91D, *Electrochim. Acta*, 2006, **51**(14), p 2898–2908
16. A.T. Kuhn, Plasma anodized aluminum—A 2000/2000 Ceramic Coating, *Met. Fnish.*, 2002, **100**(11–12), p 44
17. X. Nie, E.I. Meletis, J.C. Jiang, A. Leyland, A.L. Yerokhin, and A. Matthews, Abrasive Wear/Corrosion Properties and TEM Analysis of Al_2O_3 Coatings Fabricated Using Plasma Electrolysis, *Surf. Coat. Technol.*, 2002, **149**(2–3), p 245–251
18. R.C. Barik, J.A. Wharton, R.J.K. Wood, K.R. Stokes, and R.L. Jones, Corrosion, Erosion and Erosion–Corrosion Performance of Plasma Electrolytic Oxidation (PEO) Deposited Al_2O_3 Coatings, *Surf. Coat. Technol.*, 2005, **199**(2–3), p 158–167
19. Y. Guangliang, L. Xianyi, B. Yizhen, C. Haifeng, and J. Zengsun, The Effects of Current Density on the Phase Composition and Microstructure Properties of Micro-arc Oxidation Coating, *J. Alloy Compd.*, 2002, **345**(1–2), p 196–200
20. J.A. Curran and T.W. Clyne, Porosity in Plasma Electrolytic Oxide Coatings, *Acta Mater.*, 2006, **54**(7), p 1985–1993
21. L. Rama Krishna, A. Sudha Purnima, and G. Sundararajan, A Comparative Study of Tribological Behavior of Microarc Oxidation and Hard-anodized Coatings, *Wear*, 2006, **261**(10), p 1095–1101
22. L. Rama Krishna, A.V. Rybalco, and G. Sundararajan, US Patent No. 6,893,551
23. M. Stern and A.L. Geary, Electrochemical Polarization, 1. A Theoretical Analysis of the Shape of Polarization Curves, *J. Electrochem. Soc.*, 1957, **104**(12), p 751–752
24. W.A. Badawy, F.M. Al-Kharafi, and A.S. El-Azab, Electrochemical Behaviour and Corrosion Inhibition of Al, Al-6061 and Al–Cu in Neutral Aqueous Solutions, *Corr. Sci.*, 1999, **41**(4), p 709–727
25. P.R. Roberge (Ed.), *Handbook of Corrosion Engineering*, McGraw-Hill, 1999, p 341
26. A. Alavi and R.A. Cottis, The Determination of pH, Potential and Chloride Concentration in Corroding Crevices on 304 Stainless Steel and 7475 Aluminium Alloy, *Corr. Sci.*, 1987, **27**(5), p 443–451
27. N. Lampeas and P.G. Koutsoukos, The Importance of the Solution pH in Electrochemical Studies of Aluminium in Aqueous Media containing Chloride, *Corr. Sci.*, 1994, **367**(5), p 1011–1025
28. R.D. Armstrong and V.J. Braham, The Mechanism of Aluminium Corrosion in Alkaline Solutions, *Corr. Sci.*, 1996, **38**(9), p 1463–1471
29. A.V.C. Sobral, W. Ristow, D.S. Azambuja, I. Costa, and C.V. Franco, Potentiodynamic Tests and Electrochemical Impedance Spectroscopy of Injection Molded 316L Steel in NaCl Solution, *Corr. Sci.*, 2001, **43**(6), p 1019–1030
30. H. Wu, X. Zang, and K.R. Hebert, Atomic Force Microscopy Study of the Initial Stages of Anodic Oxidation of Aluminum in Phosphoric Acid Solution, *J. Electrochem. Soc.*, 2000, **147**(6), p 2126–2132
31. J.J. Suay, E. Giménez, T. Rodríguez, K. Habbib, and J.J. Saura, Characterization of Anodized and Sealed Aluminium by EIS, *Corr. Sci.*, 2003, **45**(3), p 611–624